RESEARCH ARTICLE

Developmental Dynamics WILEY

Distinct regulatory states control the elongation of individual skeletal rods in the sea urchin embryo

Kristina Tarsis | **Tsvia Gildor** | **Miri Morgulis** | **Smadar Ben-Tabou de-Leon** [ID]

Department of Marine Biology, Leon H. Charney School of Marine Sciences, University of Haifa, Haifa, Israel

Correspondence
Smadar Ben-Tabou de-Leon, Department of Marine Biology, Leon H. Charney School of Marine Sciences, University of Haifa, Haifa 31905, Israel.
Email: sben-tab@univ.haifa.ac.il

Abstract

Background: Understanding how gene regulatory networks (GRNs) control developmental progression is a key to the mechanistic understanding of morphogenesis. The sea urchin larval skeletogenesis provides an excellent platform to tackle this question. In the early stages of sea urchin skeletogenesis, skeletogenic genes are uniformly expressed in the skeletogenic lineage. Yet, during skeletal elongation, skeletogenic genes are expressed in distinct spatial sub-domains. The regulation of differential gene expression during late skeletogenesis is not well understood.

Results: Here we reveal the dynamic expression of the skeletogenic regulatory genes that define a specific regulatory state for each pair of skeletal rods, in the sea urchin *Paracentrotus lividus*. The vascular endothelial growth factor (VEGF) signaling, essential for skeleton formation, specifically controls the migration of cells that form the postoral and distal anterolateral skeletogenic rods. VEGF signaling also controls the expression of regulatory genes in cells at the tips of the postoral rods, including the transcription factors Pitx1 and MyoD1. Pitx1 activity is required for normal skeletal elongation and for the expression of some of VEGF target genes.

Conclusions: Our study illuminates the fine-tuning of the regulatory system during the transition from early to late skeletogenesis that gives rise to rod-specific regulatory states.

KEYWORDS
biomineralization, gene regulatory networks, MyoD, Pitx, sea urchin, skeletogenesis, vascular endothelial growth factor

1 | INTRODUCTION

Transcription factors, signaling molecules, and regulatory RNAs form gene regulatory networks (GRNs) that drive cell fate specification during embryogenesis.[1-3] The GRNs control the regulatory state of the cells, which is the specific combination of transcription factors within the cell nucleus.[4] The regulatory states define which genes are activated and which genes are repressed and by that drive cell fate specification and morphogenesis. As development progresses, successive cascades of regulatory genes are activated: early regulatory genes activate

the expression of late regulatory genes and enable the refinement of regulatory states, cell fate, and function.[1,5] Understanding how early GRNs activate the late, elaborate GRNs and how these regulatory cascades encode developmental progression is a key to the understanding of the genetic regulation of morphogenesis.

Sea urchin larval skeletogenesis is a prominent model for dissecting the genetic regulation of developmental progression.[5–12] The larval skeleton of the sea urchin is made of two calcite rods, the spicules, that are engulfed within a tubular spicule cavity, generated by the skeletogenic cells.[5,7,13] During embryogenesis, the skeletogenic cells go through epithelial to mesenchymal transition and enter the blastocoel, fuse through their filopodia and form a pseudopodia cable that links them into a syncytium (Figure 1A).[13,14] The skeletogenic cells organize in a ring with two ventrolateral cell clusters in which the tri-radiate spicules form (Figure 1A, I[17–19]). The spicules elongate within the pseudopodia cable and generate the body, anterolateral and mid-ventral rods (Figure 1A). A set of skeletogenic cells then migrate from

the ventrolateral clusters and guide the elongation of the postoral rods; skeletogenic cells from the longitudinal chain migrate to form the distal part of the anterolateral rods (Figure 1A,B). The growth rate differs between the rods, and particularly, the postoral rod is the last to grow but has the fastest elongation rate.[20] The spicule rods grow rapidly at their tips and slower at their girth, suggesting that mineral deposition is enhanced at the growing spicule tips compared to the back.[21] Relatedly, as the spicules elongate, the expression of some skeletogenic genes becomes restricted to the cells proximal to the growing tips, possibly to enhance spicule growth at these sites (Figure 1C).[21–23] As all the skeletogenic cells are connected through their cytoplasm, the regulation of localized gene expression within the skeletogenic-syncytium is quite intriguing.

A prominent regulator of skeletal growth and gene expression is the vascular endothelial growth factor (VEGF) signaling pathway.[7,11,15,16,21,23] At the gastrula stage, the VEGF ligand is secreted from two lateral ectodermal domains while the VEGF receptor (VEGFR) is
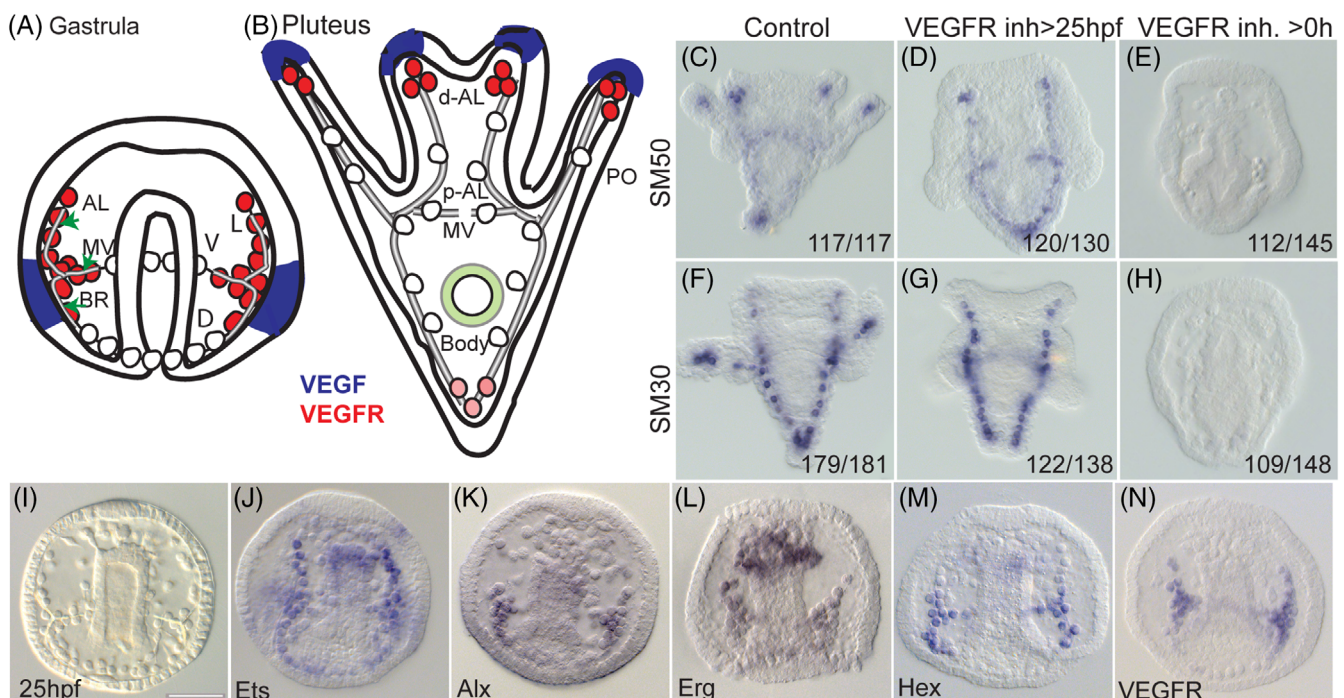

FIGURE 1 Sea urchin larval skeletogenesis and gene expression. (A) Sea urchin embryo at the gastrula stage. AL, anterolateral rods; MV, mid-ventral rods; BR, body rods; D, dorsal skeletogenic chain; L, longitudinal skeletogenic chain; V, ventral skeletogenic chain. The pseudopodia cable between the skeletogenic cells is marked in black lines. VEGFR expression is marked in red and VEGF is marked in blue, based on.[15,16] (B) Sea urchin embryo at the pluteus stage. PO, postoral rods; p-AL, proximal anterolateral rods; d-AL, distal anterolateral rods. (C-H) Differential expression of SM50 and SM30 at 2 dpf and the effect of VEGFR continuous and late inhibition. (C-E) SM50 expression in control (C), late VEGFR inhibition (D), and continuous VEGFR inhibition (E). (F-H) SM50 expression in control (F), late VEGFR inhibition (G), and continuous VEGFR inhibition (H). Numbers at the bottom indicate the number of embryos that show this phenotype (left) out of all embryos scored (right), conducted in three independent biological replicates. (I-N) Embryo morphology and gene expression at the time of the addition of VEGFR inhibitor (25 hpf) in the late inhibition experiments. (I) Embryo morphology, arrowheads point to the tri-radiate spicules. Gene names are indicated at the bottom in (J-N)

expressed in the neighboring skeletogenic cells, where active spicule growth occurs (Figure 1A, N[15,16]). Inhibition of sea urchin VEGF signaling by genetic manipulation or using the VEGFR-specific inhibitor, axitinib, distorts skeletogenic cell migration and completely blocks spicule formation.[7,16,21] At the pluteus stage, VEGFR is expressed at the tips of the postoral and anterolateral rods, and VEGF is expressed at the ectodermal cells near these tips (Figure 1B[15,16]). A weak expression of VEGFR is also observed at the tips of the body rods, but VEGF is not expressed near these cells.[15] Accordingly, late inhibition of VEGF signaling inhibits the elongation of the postoral and distal anterolateral rods and downregulates the expression of skeletogenic genes at the tips of these rods, but not at the body rods (Figure 1C-H[21–23]). Thus, VEGF signaling is one of the factors regulating localized gene expression and directing spicule growth, yet, little is known about the regulatory states at the tips of the rods and the mechanisms that mediate the transcriptional response to VEGF signaling.

We recently studied the molecular machinery activated by the VEGF pathway during sea urchin skeletogenesis and discovered hundreds of genes that respond to VEGFR inhibition, including regulatory and vascularization-related genes.[7] Moreover, five upstream transcription factors and three signaling genes that drive skeletogenesis are homologous to vertebrate factors that control vascularization.[6,7,24] The VEGF pathway participates in biomineralization in all studied echinoderms[15,16,25–27] while in many other phyla it controls tubulogenesis and prominently, vascularization.[24,28–31] This led us to propose that sea urchin skeletogenesis and vertebrate vascularization diverged from a common ancestral tubulogenesis program, uniquely co-opted for biomineralization in the echinoderm phylum.[7,24]

Two of the genes that respond most significantly to VEGF inhibition encode the transcription factors, MyoD1 and Pitx1 that could have a role in the regulation of skeletogenic gene expression.[7] Sea urchin Pitx1 is a homolog of the vertebrates' Pitx family of paired-related homeodomain transcription factors that regulate the formation of multiple organs, including biomineralization-related processes such as teeth and hindlimb development.[32–41] MyoD1 is a sea urchin homolog of the vertebrates MyoD family of basic helix loop helix (bHLH) transcription factors that are typically involved in myogenic determination and differentiation.[42] Interestingly, Pitx2 and genes from the MyoD family cooperate to regulate skeletal muscle differentiation in vertebrates.[42] However, sea urchin Pitx1 and MyoD1 are not a part of the myogenesis regulatory network in the sea urchin embryo[43] and are exclusively expressed in skeletogenic cells downstream of VEGF signaling.[7] The expression

and role of these genes in late sea urchin skeletogenesis were not studied before.

While the GRN that controls the early stages of skeletogenesis is known in great details,[6,8,10–12,44] the regulatory states and mechanisms that control skeletal elongation and differential gene expression are not fully understood. Here we investigate the expression of key skeletal regulatory genes and their response to early and late perturbations of VEGF signaling during skeletal elongation. We study the dynamic expression pattern of *Pitx1* and *MyoD1* and the role of the transcription factor Pitx1 in skeletal elongation and regulation of skeletogenic gene expression. Our studies portray the transition between the initial regulation of spicule formation to the intricate regulation of the growth of individual skeletal rods.

2 | RESULTS

2.1 | Rod-specific regulatory states are formed during skeletal elongation and postoral gene expression depends on late VEGF signaling

To illuminate the regulatory states that form in the skeletogenic lineage during skeletal elongation, we studied the spatial expression of key skeletogenic regulatory genes at the prism and pluteus stages, in control embryos and under late and continuous VEGFR inhibition (Figures 2 and 3). In continuous VEGFR inhibition, the embryos are grown with VEGFR inhibitor, axitinib, from the time of fertilization and on, which causes complete loss of skeletal growth and a highly irregular positioning of the skeletogenic cells (Figures 2A,B and 3A,B), in agreement with previous studies.[15,16] In late VEGFR inhibition, the inhibitor is added at 25 h post-fertilization (hpf), which is after the skeletogenic cells are arranged in a ring with two ventrolateral cells clusters and just after the spicule first forms (Figure 1I). Late VEGFR inhibition does not interfere with the growth of the body rods, but prevents cell migration required for the generation of the postoral rods and the elongation of the distal part of the anterolateral rods (Figures 2 and 3, panels A, B), in agreement with previous studies in other sea urchin species.[16,21]

We studied the expression of early and late skeletogenic transcription factors and signaling molecules responsible for different functions in the skeletogenic cells. The transcription factors Ets1/2, Alx1, Erg, and Hex drive early skeletogenic cell specification,[6,10,44,45] are necessary for the skeletogenic epithelial to mesenchymal transition[46] and represent the early upstream skeletogenic GRN. At
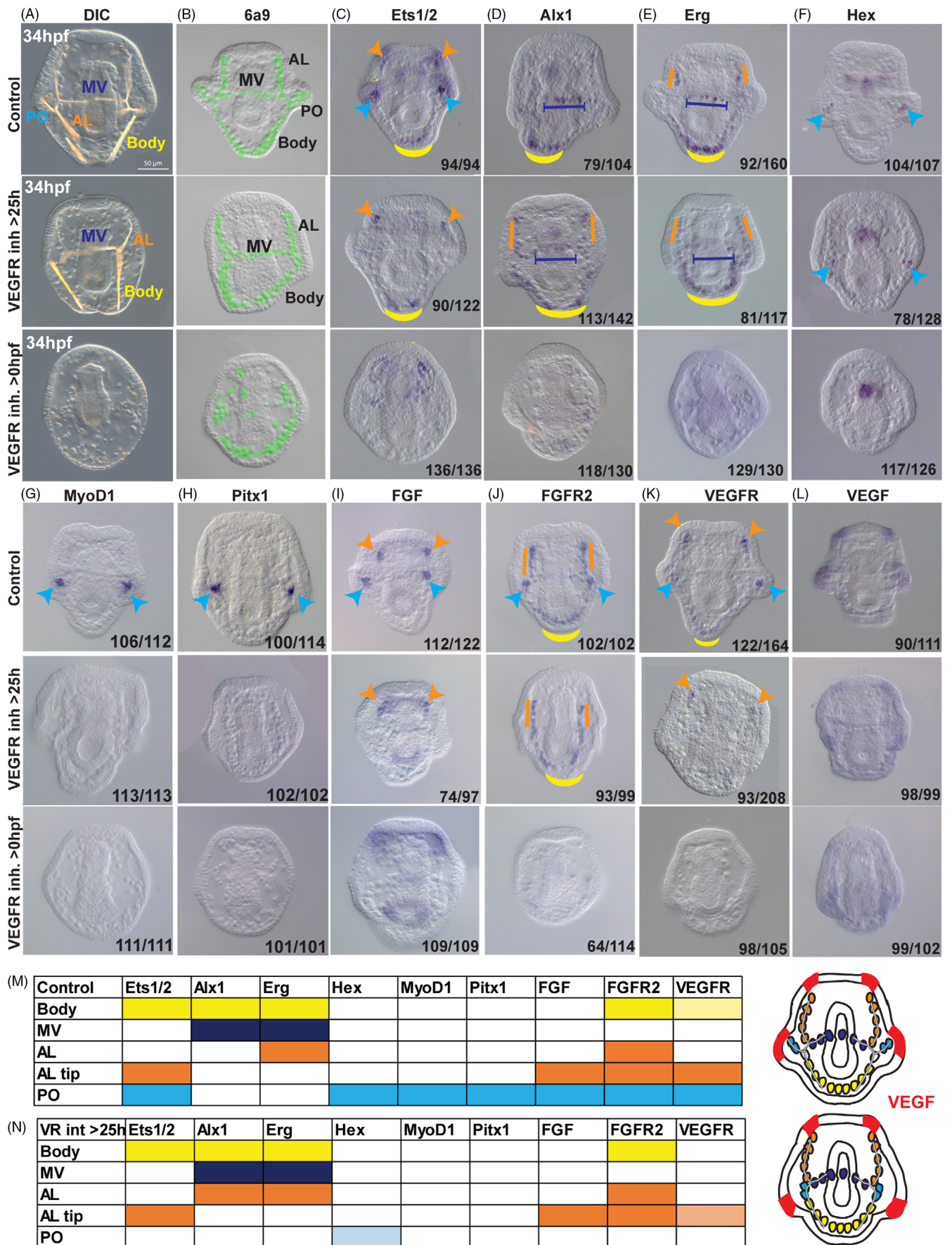
FIGURE 2 Legend on next page.

the time of the addition of VEGFR inhibitor, these genes are expressed in the skeletogenic cells and their expression is enriched at the skeletogenic lateral cell clusters (Figure 1J-M). The fibroblast growth factor (FGF) and its receptor, FGFR2, are expressed in the skeletogenic cells after they ingress into the blastocoel and are important for skeletal elongation.[16,47] We also studied the transcription factors Pitx1 and MyoD1, the ligand, VEGF, and the receptor, VEGFR, mentioned above.

The skeletogenic regulatory genes form distinct regulatory states at the tips of each pair of rods and the expression at the tips of the postoral rods strongly depends on late VEGF signaling. The most dorsal cells of the body rods express the genes encoding the transcription factors Ets1/2, Alx1, and Erg and the signaling receptor, FGFR2, at the prism and pluteus stages, independently of late VEGF signaling (Figures 2 and 3, panels C-E,J,M,N). The expression of Alx1 in skeletogenic cells at the tips of the body rods was also observed in Sun and Ettenshon [21] and Chang and Su .[23] A faint expression of VEGFR2 is detected in these cells at both time points and is reduced under VEGFR inhibition (Figures 2 and 3, panels K,M,N). The cells along the mid-ventral rods express the genes encoding the transcription factors Alx1 and Erg at the prism and pluteus stages, independently of late VEGF signaling (Figures 2 and 3, panels D,E,M,N). The cells at the tips of the anterolateral rods express the transcription factors Ets1/2 and the signaling molecular FGF, FGFR2, and VEGFR, at the prism and pluteus stages (Figures 2 and 3 panels C,J-K,M). Ets1/2 expression at the tips of the anterolateral rods was also observed in Chang and Su.[23] The expression of *VEGFR* in this domain is reduced in late VEGFR inhibition while the expression of the other regulatory genes is unchanged (Figures 2 and 3 panels C,J-K,N). The expression of *erg* and *FGFR2* is observed in cells along the anterolateral rods at the prism stage, in both control and late VEGFR inhibition, and the expression of *alx1* is detected in this domain only in late VEGFR inhibition, suggesting an inhibitory role of VEGF signaling on *alx1* (Figure 1D,E,J-K,M,N). The cells at the tips of the postoral rods express

the genes encoding the transcription factors Ets1/2, Hex, MyoD1 and Pitx1 and the signaling molecules, FGF, FGFR2, and VEGFR2, and the expression of all these genes strongly depends on late VEGF signaling (Figures 2 and 3 panels C, F-K, M, N).

In contrast to the specific effect of late VEGFR inhibition, continuous inhibition of VEGFR eliminates the expression of most of the genes in prism and pluteus stages, except from *ets1/2*, *alx1* and *erg* expressed in scattered skeletogenic cells in this condition (Figures 2 and 3, panels C-K). The expression of the ligand, VEGF, did not show a distinct change under VEGFR inhibition (Figures 2 and 3L). Thus, at the prism and pluteus stages, the expression of skeletogenic regulatory genes is localized at specific skeletogenic cells forming distinct regulatory states of which, the regulatory state at the tips of the postoral rods requires late VEGF signaling.

2.2 | Late VEGF signaling mildly affects the expression of VEGF targets but is essential for *pitx1* and *myoD1* expression

Late VEGF signaling has a milder effect on the expression of the skeletogenic regulatory genes compared to continuous VEGF inhibition (Figures 2 and 3), hence we wanted to study the differences between these two treatments on the expression of VEGF target genes at the pluteus stage. We tested the effect of VEGFR inhibition on the expression levels of genes encoding the receptor, VEGFR, the transcription factors Pitx1 and MyoD1, the spicule matrix protein SM30, and the cytoskeleton remodeling protein Rhogap24l/2. SM30 is one of the most abundant matrix proteins found occluded in the sea urchin spicules.[48,49] Rhogap24l/2 is a GTPase-activating protein that is expressed in the skeletogenic cells and its perturbation leads to ectopic spicule branching.[7] All these genes were shown to depend on VEGF signaling at the gastrula stage[7,15,16,23] and here we studied the effect of VEGFR inhibition on their expression levels at the pluteus stage, 2 and 3 days post-fertilization (dpf).

FIGURE 2 Differential expression of the skeletogenic regulatory genes at prism stage and the effect of VEGFR continuous and late inhibition. (A-L) Representative images of control embryo (top panels), embryos where VEGFR inhibitor, axitinib, was added at 25 hpf (middle panels), and embryos that were exposed to continuous VEGFR inhibition (bottom panels), at the prism stage (~34 hpf in *Paracentrotus lividus*). (A) DIC images, scale bar indicates 50 μm. MV, mid-ventral; AL, anterolateral; PO, postoral rods. (B) Skeletogenic cell marker, 6a9. (C-L) Gene names are indicated at the top of each panel. Arrowheads point to expression at the tips of the AL rods (orange) and PO rods (cyan). Yellow arcs show the expression at the body rods, lines showing expression along the AL rods (orange) or the MV rods (dark blue). Numbers at the bottom of each image in (C-L) indicate the number of embryos that show this phenotype (left) out of all embryos scored (right), conducted in at least three independent biological replicates. (M, N) Tables summarizing gene expression in control embryos (M) and under late VEGFR inhibition (N) at the different skeletogenic domains (left), illustrated in an embryo diagram (right). Similar color codes are used throughout the figure
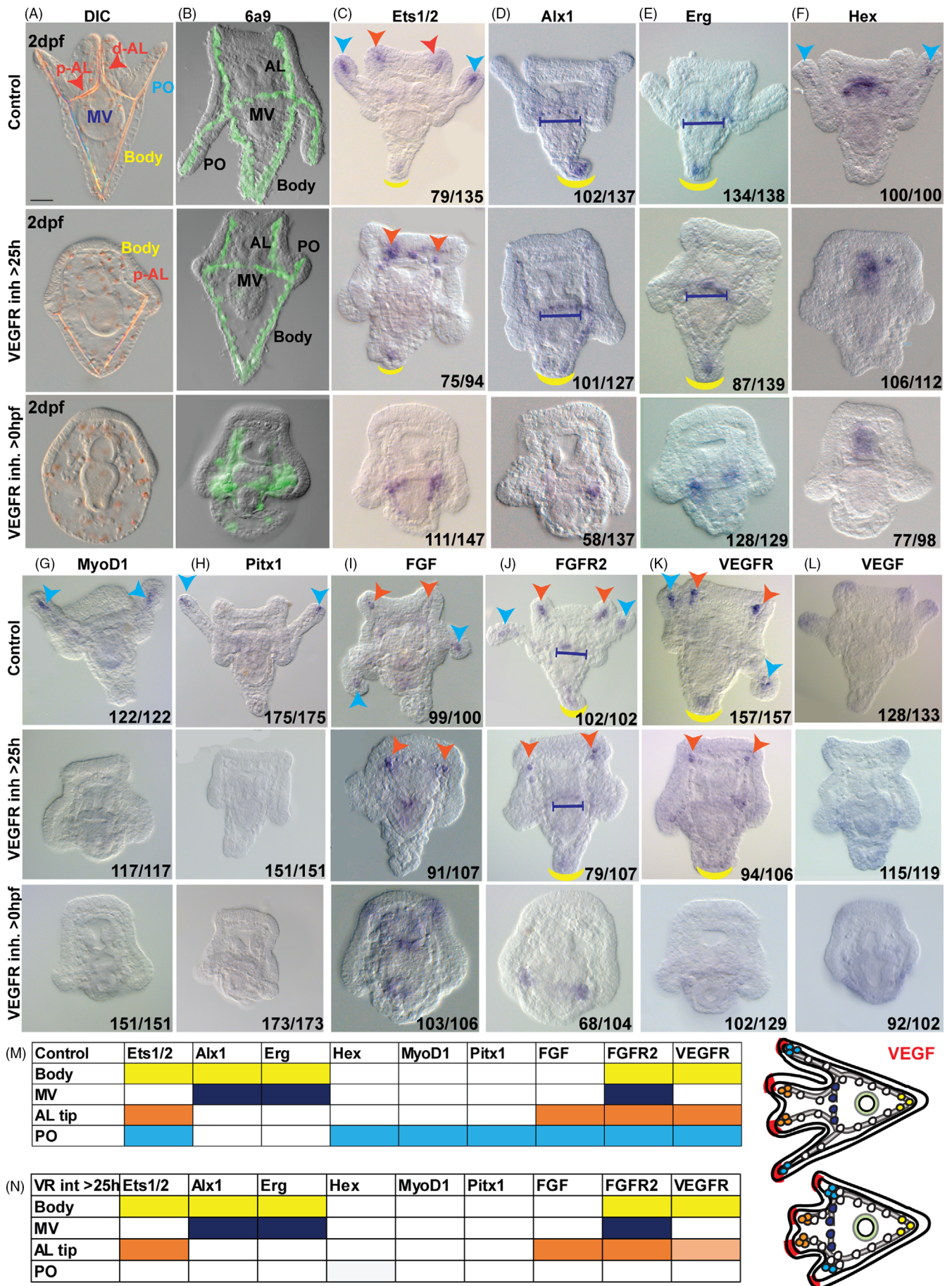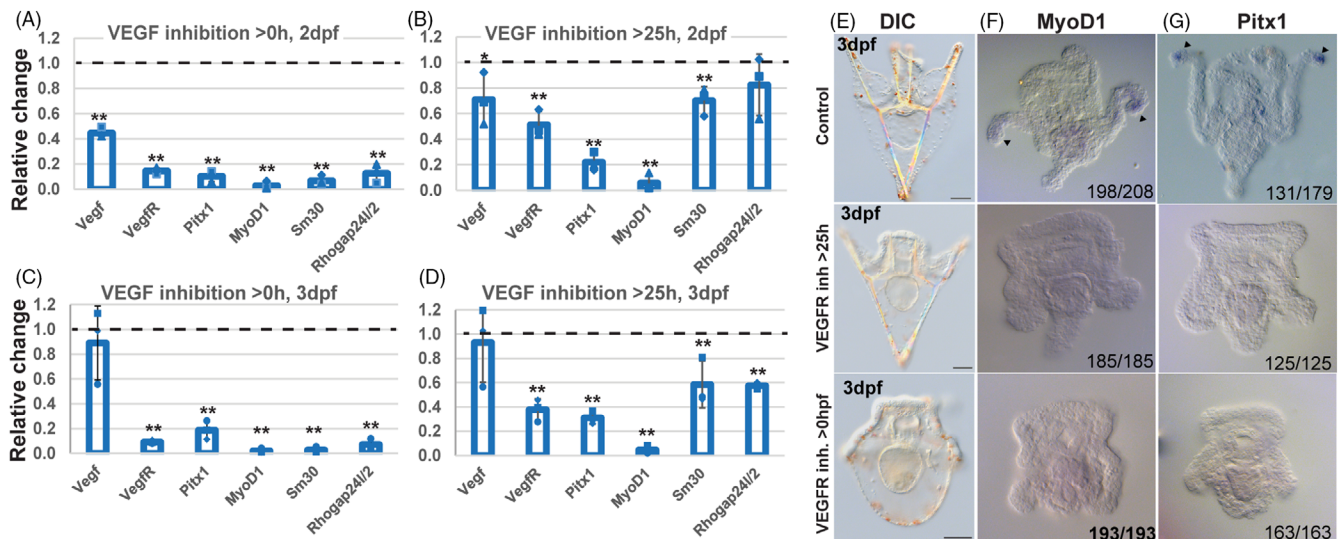
FIGURE 3 Legend on next page.

FIGURE 4 Effect of VEGFR inhibition on skeletal growth and gene expression in the pluteus stage. (A-D) Relative gene expression levels of treated embryos vs control embryos measured by QPCR at 2 dpf (A,B) and at 3 dpf (C,D). (A, C) Showing results for continuous VEGFR inhibition (>0 hpf) and (B, D) showing results for late VEGFR inhibition (>25 hpf). Bars show averages over three independent biological replicates and markers indicate individual repeats. Ratio of 1 indicates that the expression of the gene is unaffected by VEGFR inhibition. Error bars indicate SD. The significance was calculated by one-tailed z-test. One star represents $P < .01$ and two stars represent $P < .001$. (E-G) Representative embryos at 3 dpf showing skeletogenic phenotypes (E), myoD1 (F), and pitx1 gene expression (G). In each panel, we present control embryo (top), embryo in late VEGFR inhibition (>25 hpf, middle), and embryo where VEGFR was continuously inhibited (>0 hpf, bottom). Embryos are oriented similarly along the dorsal-ventral axis where the dorsal side is at the bottom, scale bars indicate 50 μm. Arrowheads point to expression at the tips of the PO rods. Numbers at the bottom of each representative image in (F, G) indicate the number of embryos that show this phenotype (left) out of all embryos scored (right), conducted in three independent biological replicates

We found a distinct difference in the transcriptional response of VEGF targets between continuous and late inhibition of VEGF signaling at 2 dpf and 3 dpf (Figure 4A-D). Continuous VEGFR inhibition reduces the expression of all tested skeletogenic genes to less than 20% of their expression in control embryos (Figure 4A,C). This agrees with the strong effect of this perturbation on the spatial expression of the skeletogenic regulatory genes at the pluteus stage (Figure 3). However, late inhibition of VEGF signaling reduces the expression of the genes by less than 50% of their normal expression at 2 dpf and 3 dpf, except for the genes that encode the transcription factors Pitx1 and MyoD1, which show stronger reduction (Figure 4B,D). These results agree with the effect of late VEGFR inhibition on the expression of the skeletogenic regulatory genes that mostly affect the expression at the postoral rods, where *pitx1* and *myoD1* are exclusively expressed at the pluteus stage (Figures 3). To complete this set of experiments, we studied the spatial expression of these two genes and the effect of VEGFR inhibition at 3 dpf (Figure 4E-G). Skeletogenesis does not recover in continuous VEGFR inhibition at 3 dpf, but the only effect of late VEGFR inhibition is a delayed elongation of the postoral and the anterolateral rods (Figure 4E). At this time, *myoD1* and *pitx1* are expressed within a few skeletogenic cells at the tips of postoral rods and their expression is completely abolished in both, continuous and late inhibition of VEGF signaling (Figure 4F,G).

FIGURE 3 Differential expression of the skeletogenic regulatory genes at pluteus stage and the effect of VEGFR continuous and late inhibition. (A-L) Representative images of control embryos (top panels), embryos where VEGFR inhibitor was added at 25 hpf (middle panels), and embryos exposed to continuous VEGFR inhibition (bottom panel). Embryos are at the pluteus stage (∼2 dpf). (A) DIC images, scale bar indicates 50 μm. Rod names are like in Figure 1B and color code is like in Figure 2. (B) Skeletogenic cell marker, 6a9. (C-L) Gene names are indicated at the top of each panel. Numbers at the bottom of each representative image in (C-L) indicate the number of embryos that show this phenotype (left) out of all embryos scored (right). Experiments were conducted in three independent biological replicates for all genes. (M, N) Tables summarizing gene expression in control embryos (M) and under late VEGFR inhibition (N) at the different skeletogenic domains (left), illustrated in an embryo diagram (right)

To investigate *pitx1* and *myoD1* spatio-temporal expression throughout skeletogenesis we studied their expression every few hours from gastrula to pluteus stage (Figure 5). At the time of skeletal initiation, both genes are expressed within the skeletogenic ventrolateral clusters as previously reported (24 hpf, Figure 5A,I[7]). At 27-32 hpf, *myoD1* remains localized at the ventrolateral cell clusters (Figure 5B-D) while the expression of *pitx1* expands to neighboring cells, and is observed within the dorsal, longitudinal, and ventral skeletogenic chains (Figure 5J-L). From prism to pluteus stages (34-44 hpf), the expression of *pitx1* becomes localized to cells at the tips of the growing postoral rods (Figure 5M-P), which is similar to the expression of *myoD1* at the same time points (Figure 5E-H). Thus, after the initial activation of *pitx1* and *myoD1* in the lateral skeletogenic cells clusters, the expression *pitx1* expression expands while *myoD1* expression remains localized. Later the expression of both genes is localized in the migrating cells at the tips of the growing postoral rods.
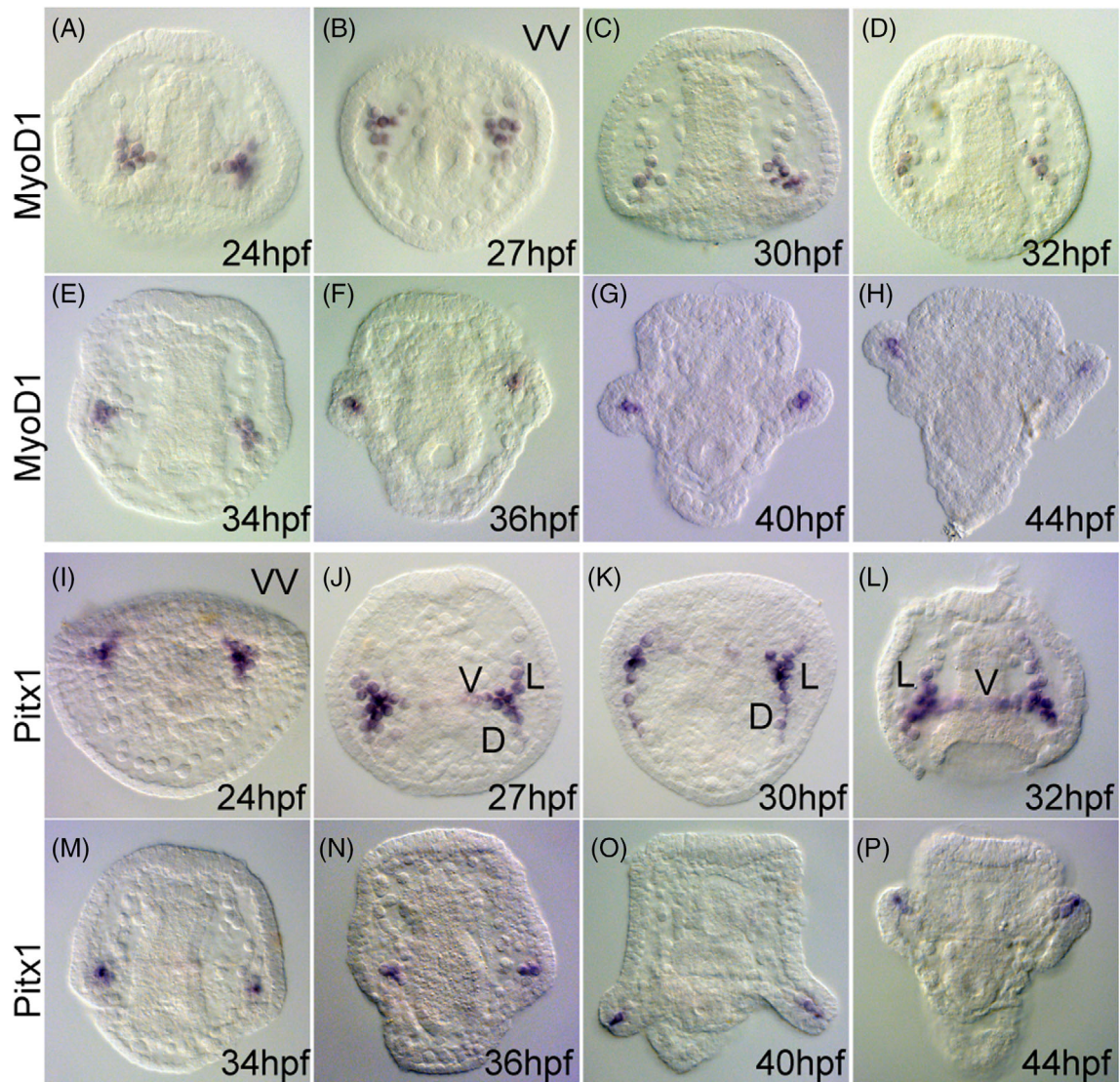

FIGURE 5 Spatiotemporal expression of *myoD1* and *pitx1* from gastrula to *pluteus* stage (24-44 hpf). (A-H) *myoD1* spatiotemporal expression. During the gastrula, stage *myoD1* is expressed at the skeletogenic ventrolateral clusters (A-D). At prism and pluteus stages, *myoD1* is expressed at the cells at the tips of the growing postoral rods (E-H). (I-P) *pitx1* spatiotemporal expression. At the early gastrula stage, *pitx1* is expressed at the skeletogenic ventrolateral clusters (I). (J-L) During late gastrula stage, *pitx1* is expressed within cells of dorsal (D), longitudinal (L), and ventral (V) chains. At prism stage (M, N) shrinks to the cells that form the postoral rods and is expressed at the tips of these rods in pluteus stage (O-P). Embryos at the gastrula stage are presented in lateral view except A and J where they are presented in ventral view (VV). At the prism and pluteus stages embryos are presented in the same orientation along the dorsal-ventral axis where the dorsal side is at the bottom of the image

2.3 | Downregulation of *pitx1* causes a significant reduction in elongation of the skeletal rods

The dynamic spatial expression of the *pitx1* gene and its strong dependence on VEGF signaling motivated us to study its role in sea urchin skeletogenesis. To do that we knocked-down the expression of *pitx1* by microinjection of two different morpholino antisense oligonucleotides (MOs) targeted to block the splicing of the gene at two distinct exons (Figure 6A). Random MO was injected as a control. To test the activity of the two MOs we designed polymerase chain reaction (PCR) primers that distinguish between the full transcripts and the truncated transcripts for each MO (Figure 6B,C). PCR on cDNA synthesized from uninjected embryos and from embryos injected with random MO produces one band that corresponds to the full transcript (Figure 6D,E, see Experimental Procedures for details). PCR of cDNA synthesized from embryos injected with sMO1 produces two bands that correspond to the truncated transcripts and the full transcript (Figure 6D). PCR on cDNA of embryos injected with

sMO2 shows a single strong band of a truncated transcript (Figure 6E). This data confirms that both MOs block normal splicing as expected; however, sMO2 seems to be more efficient in inhibiting normal splicing of the *pitx1* transcript.

Downregulation of *pitx1* interferes with skeletal elongation and results in shorter skeletal rods at 3 dpf, as exemplified with representative embryos in Figure 7A-C. To quantify the effect, we measured the length of each rod in embryos injected with *pitx1* sMOs and in embryos injected with random MO as control (Figure 7D, see Experimental Procedures for details). The injections of both sMOs result in a significant decrease in the length of postoral, body, and distal anterolateral (d-AL) rods, with minor differences in the activity between the two sMOs (Figure 7E,F,H). The length of proximal anterolateral (p-AL) rods has been significantly decreased in sMO2 injected embryos but not in sMO1 (Figure 7G), possibly since sMO1 is less effective than sMO2 in blocking the splicing of *pitx1* (Figure 6E). Overall, our findings indicate that Pitx1 is important for the normal elongation of the body, AL, and postoral skeletal rods.
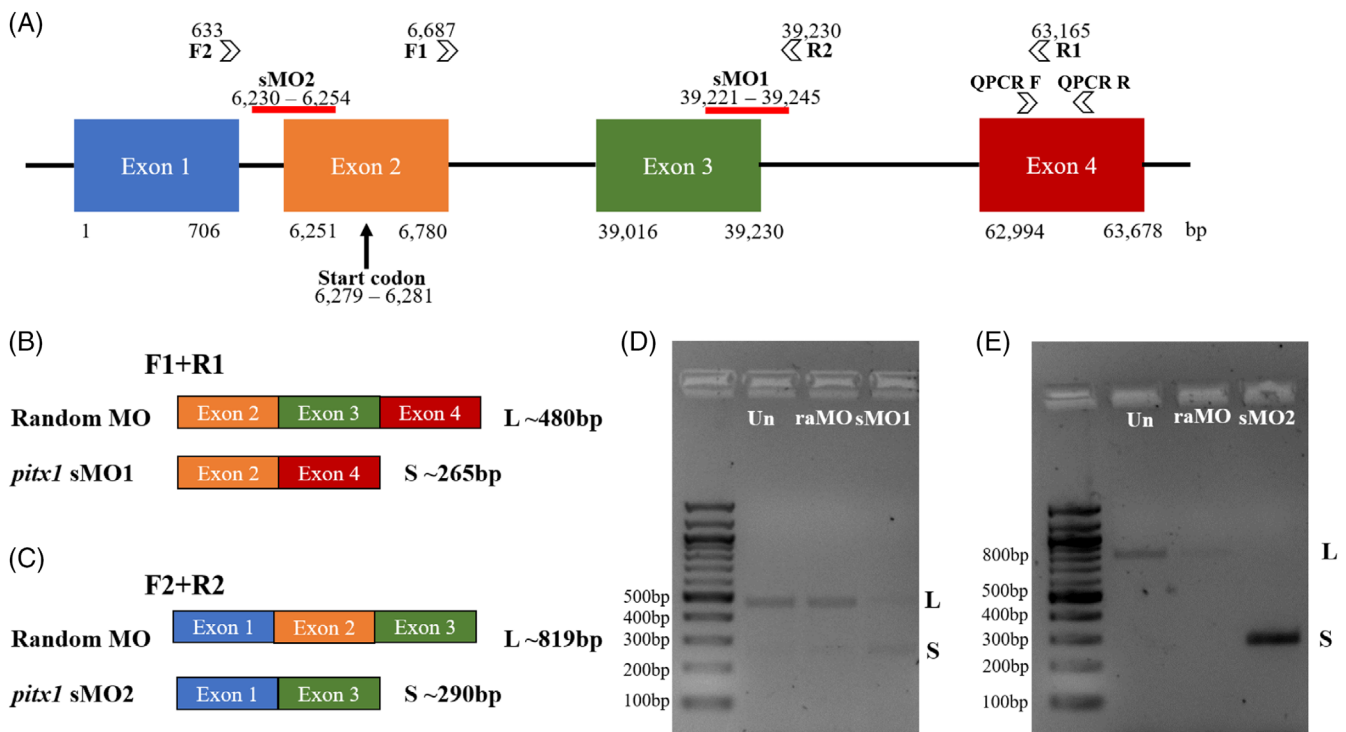

FIGURE 6 *Pl-pitx1* MO design and test of splicing MOs. (A) Structure of the *Pl-pitx1* gene with target sites for the two splicing MOs and PCR primer locations identified. The coordinates correspond to the distance from the beginning of the first exon. The QPCR primers that were used to assess *pitx1* level in *pitx1* perturbation experiments are located at the fourth exon, a region that is unaffected by the splicing MO. (B, C) Primer design for testing the activity of sMO1 (B) and sMO2 (C) showing the expected PCR transcripts. (D, E) Gels testing sMO1 and sMO2, respectively, showing bands of a long (full) and short (truncated) transcripts. Un, uninjected embryos; raMO, embryos injected with random MO; sMO1, embryos injected with *Pl-pitx1* splicing MO1; sMO2, embryos injected with splicing MO2; L, long transcript; S, short transcript
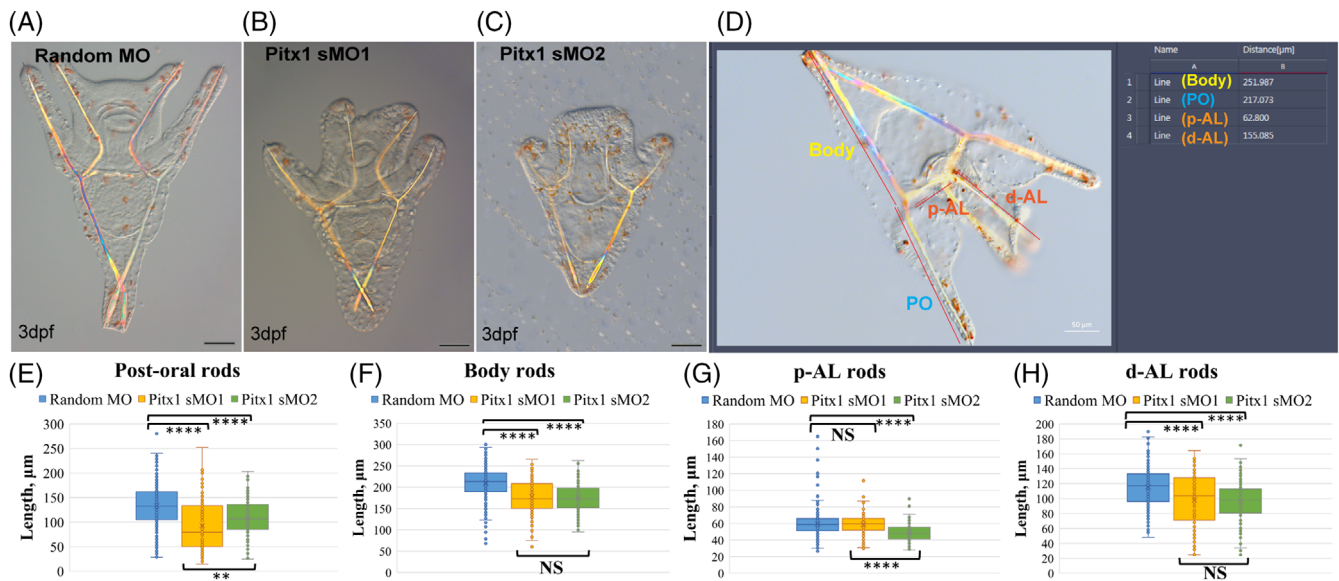
FIGURE 7 The transcription factor, Pitx1, is essential for normal skeletal elongation in the sea urchin embryo. (A-C) *pitx1* perturbations. (A) embryo injected with control (random) MO, showing normal skeleton at 3 dpf. (B, C) *pitx1* knockdown using two different splicing MOs results in short postoral, body, and distal anterolateral rods. Scale bars are 50 μm. (D) Measurement of the length of the skeletal rods. Embryos were flattened using the cover slide and the Zeiss software ZEN was used to measure the length of the different rods, as shown in the image. (E-H) Lengths of different rods in control and *pitx1* downregulated embryos. Each box plot shows an average, the first and the third quartiles (edges of boxes), and outliers (dots). Experiments were performed in 3 to 5 independent biological replicates and for each condition 99 to 115 embryos were measured. The exact number of studied embryos can be found in Table S2. *t*-test; statistical significance is represented by **$P < .01$, ****$P < .0001$

2.4 | Pitx1 perturbation affects the level but not the spatial pattern of skeletogenic gene expression

The significant effect of the perturbation of *pitx1* on the growth of all skeletal growth motivated us to study its effect on the expression of several VEGF targets. We studied the effect of *pitx1* perturbation at the early phase of its expression when it is broadly expressed within the skeletogenic cells (late gastrula, ~30-32 hpf, Figure 5K,L) and during skeletal elongation, when *pitx1* is localized to cell at the tips of the postoral rods (pluteus, 2 dpf, Figure 5P). For these experiments, we used sMO2 due to its improved efficiency in inhibiting the activity of *pitx1* (Figure 6E). To quantify the effect of *pitx1* downregulation on the level of *pitx1* expression, we used quantitative polymerase chain reaction (QPCR) primers located at the fourth exon, which is unaffected by sMO2 (Figure 6A and Table S1).

At the late gastrula stage, the skeletal morphology of *pitx1* morphants looks very similar to that of the control embryos injected with Random MO, (Figure 8A,B), and the expression level of some of VEGF targets is mildly altered (Figure 8C). Specifically, the expression of *SM30* and *VEGF* is reduced while the expression of *pitx1* itself is increased; yet these changes are minor. At the pluteus

stage, embryos injected with *pitx1* sMO2 show distinct delay in skeletal elongation compared to control embryos injected with Random MO (Figure 8J,K). The expression level of VEGF targets, *SM30*, *SM50*, and *MyoD1* is significantly reduced by 2-fold or more, and the expression of *pitx1* is upregulated (Figure 8L). The increase in the level of *pitx1* under *pitx1* downregulation at both time points suggests that Pitx1 is an auto-repressor of its own gene. That is, *pitx1* knockdown results in downregulation of the expression levels of *SM30*, *SM50*, and *MyoD1*, of a similar order as VEGFR late inhibition (Figure 4B), and a delay in the elongation of all skeletal rods at 2 dpf.

We tested the effect of *pitx1* downregulation on the spatial expression of VEGF targets at the same time points where we studied gene expression levels. We focused on the spicule matrix proteins, *SM30* and *SM50*, and on *pitx1* itself. At the gastrula stage, in control embryos injected with Random MO, *SM30* is expressed in the skeletogenic cell clusters, in the longitudinal chain, and in dorsal skeletogenic cells next to the skeletogenic cell clusters (Figure 8D). In control embryos, *SM50* is expressed in the same cells as *SM30*, but it is also expressed in the ventral skeletogenic chain (Figure 8F) and *pitx1* is expressed in the skeletogenic cell clusters and in the cells near them (Figure 8H). The downregulation of *pitx1* did not change the spatial expression
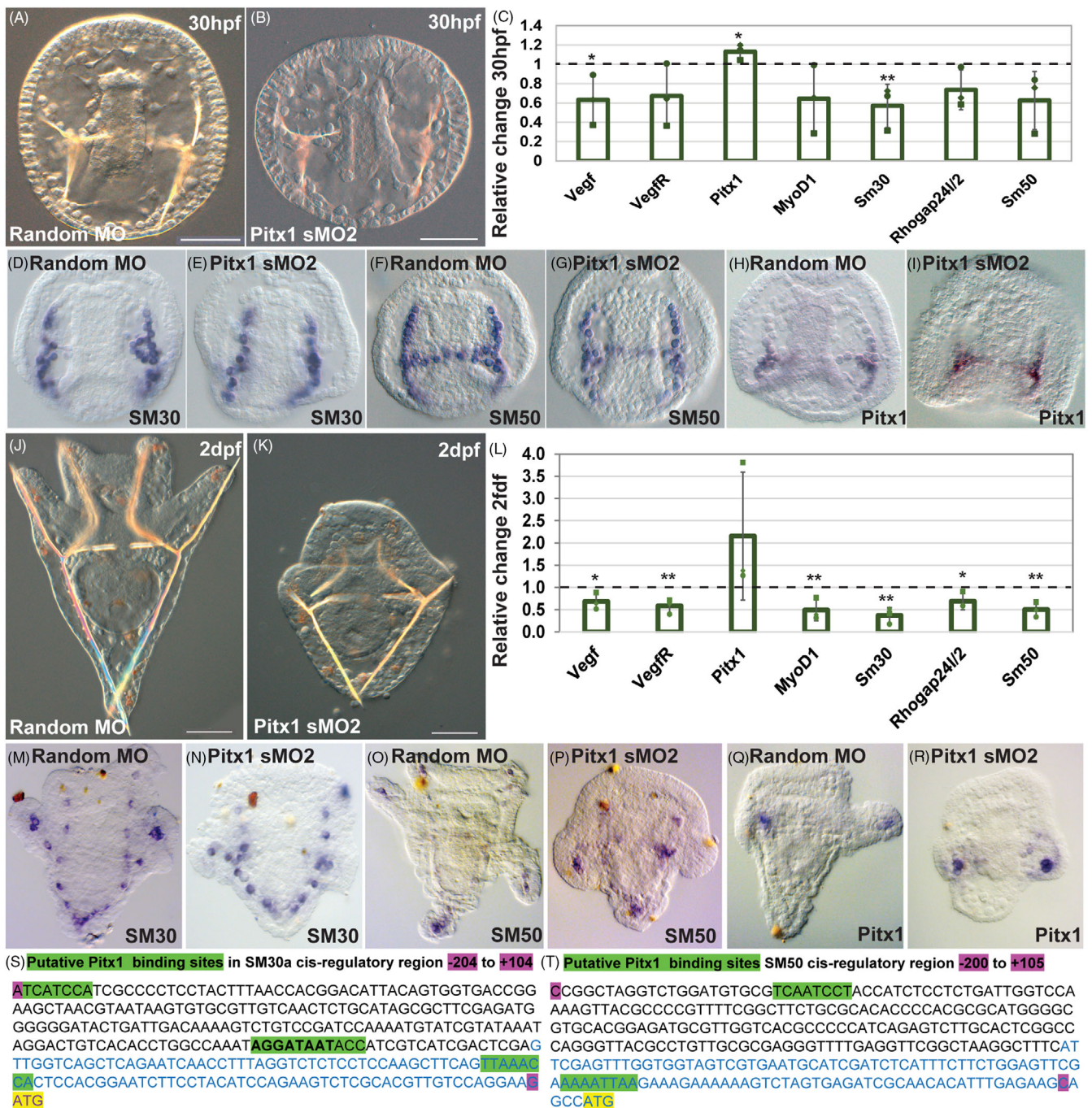
FIGURE 8 Effect of Pl-Pitx1 downregulation on gene expression at 30 hpf and 2 dpf. (A, B) Representative embryos injected with Random MO (A) and pitx1 sMO2 (B) at 30 hpf. (C) Relative change in gene expression level in pitx1 sMO2 compared to Random MO, measured by QPCR. Bars show averages and markers indicate individual measurements. Ratio of 1 (dashed line) indicates that the expression of the gene is unaffected by pitx1 downregulation. Error bars indicate SD. One-tailed z-test statistical significance is represented by *P < .01; **P < .001. (D-I) Spatial gene expression in control embryos vs embryos injected with pitx1 sMO2, gene names are indicated at the bottom. (J-R) Similar to (A-I), tested at 2 dpf. QPCR experiments were performed in 3 biological replicates and spatial expression experiments were performed in 2 to 4 biological replicates. Exact numbers of studied embryos are provided in Table S2. (T-S) Pitx putative binding sites in the promoter regions of SpSM30a (S) and SpSM50 (T), that drive expression in the skeletogenic cells.[50,51,52] Borders of active regions are marked magenta; first exon is marked in blue letters and the start of translation is highlighted in yellow. *Pitx1* putative binding sites are highlighted in green, two overlapping sites in SpSM30a are marked in bold

of these genes at this time point (Figure 8E,G,I). At the pluteus stage, in control embryos injected with Random MO, *SM30* is expressed in all the skeletogenic cells but

the ventral chain (Figure 8M), *SM50* is expressed at the tips of the body, postoral and anterolateral rods (Figure 8O) and *pitx1* is expressed at the tips of the

postoral rods (Figure 8Q). The downregulation of *pitx1* results in smaller embryos due to the skeletal delay, but did not change the spatial expression of these genes at this time (Figure 8N,P,R).

The reduction in the expression levels of *SM30* and *SM50* at the pluteus stage suggests that Pitx1 could be a direct activator of these genes. The *cis*-regulatory regions controlling the expression of *SM30* and *SM50* were characterized in the sea urchin species, *Strongylocentrotus purpuratus*,[50,51] which shows high similarity in its skeletogenic GRN and gene expression patterns to *P. lividus*.[53,54] We used human and mouse position weight matrices of Pitx1/2/3 in the Jaspar database, to identify putative binding sites in the promoter regions of *SpSM30a* and *SpSM50* that drive skeletogenic gene expression when fused to a reporter gene.[7,50,51,52] We identified four putative Pitx binding sites in the promoter regions of *SpSm30a* and two putative Pitx binding sites in the promoter region of *SpSm50* (Figure 8S,T). The function of these binding sites should be tested experimentally to confirm the direct regulation of *SM30* and *SM50* by Pitx1. Overall, our studies imply that Pitx1 acts as a transcriptional activator of the skeletogenic genes, *SM30*, *SM50*, *MyoD1*, and possibly, as a transcriptional repressor of its own gene (Figure 8).

3 | DISCUSSION

As embryo development progresses, the complexity of organs and embryonic morphology increases, and the complexity of regulatory states and GRNs that control these processes increases accordingly.[1,55] Here we studied the regulatory changes that underlie the transition between the early stage of spicule formation to the late stages of skeletal elongation in the sea urchin larva, our findings are summarized in Figure 9. We detected specific regulatory states in each pair of skeletal rods, of which, gene expression at the tips of the postoral rods requires late VEGF signaling (Figures 2, 3, and 9). There is a distinct difference between continuous and late VEGFR inhibition in the transcriptional response, except for the genes, *myoD1*, and *pitx1*, which were strongly downregulated in both treatments (Figures 2-4). The expression of these genes is first localized to the ventro-lateral skeletogenic cell clusters and later observed in cells at the tips of the growing postoral rods, and depends on VEGF signaling throughout skeletogenesis (Figures 4 and 5). Pitx1 knock-down reduces the elongation of all skeletal rods and downregulates the expression of some of VEGF targets, suggesting that this transcription factor mediates part of the transcriptional response to VEGF
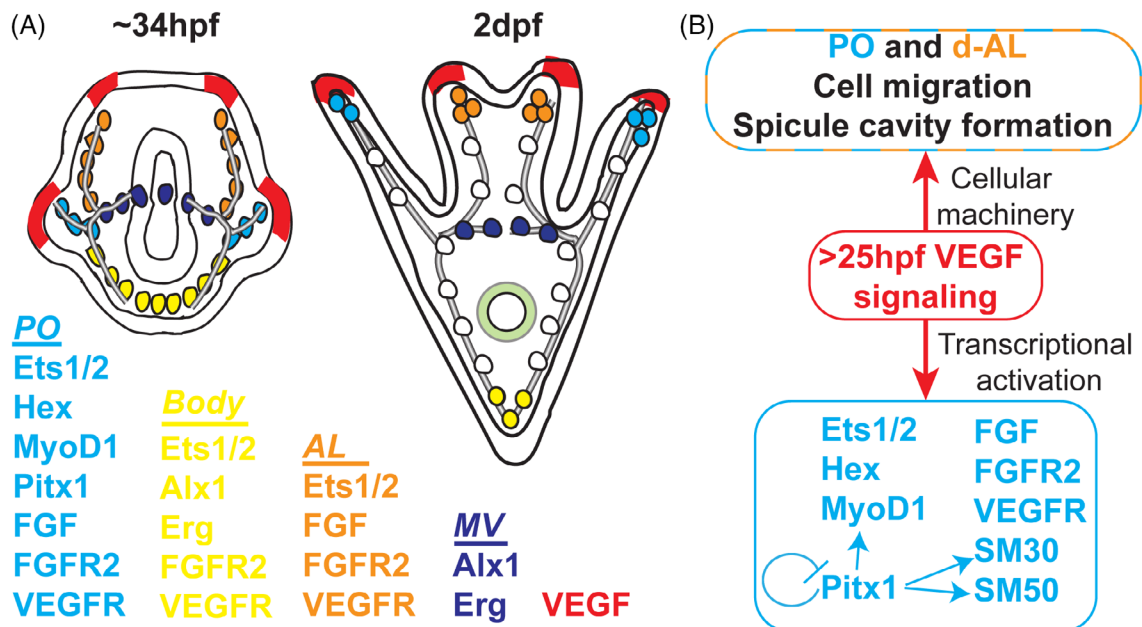

FIGURE 9 Skeletogenic regulatory states at the prism and pluteus stage and a model of the regulatory interactions in the skeletogenic lineage. (A) Embryo diagrams at the prism and pluteus stages, showing the skeletogenic cells at the body (yellow), PO (cyan), AL (orange), and MV (dark blue). The regulatory genes that are expressed within each territory are listed below using the same color code. VEGF-expressing ectodermal cells are marked in red. (B) A model of the roles of late VEGF signaling. After spicule initiation at 24 hpf, VEGF signaling is essential for the migration of the skeletogenic cells that form the PO rods and the distal AL rods and for the formation of the spicule cavity in these rods. VEGF signaling is also critical to the expression of the degulatory genes at the tips of the PO rods (cyan box). The transcription factor *Pitx1* positively regulates the expression of *SM30* and *SM50* and negatively regulates its own gene expression

signaling (Figures 6-8). Below we discuss our findings and their implications on the regulation of the transition between spicule initiation and spicule elongation.

Our studies and previous works demonstrate the specific regulatory states and GRNs that operate at the tips of the growing skeletal rods, possibly to support the distinct growth dynamics and function of these rods in the sea urchin larva (Figures 2, 3, and 9A). It was previously shown that the growth rate is rod-specific[20] and that differential gene expression is observed within the skeletogenic cell lineage after the gastrula stage.[21,23] Furthermore, the postoral and anterolateral rods form the feeding structure of the sea urchin larva that its growth and size depends on food availability[56] and could require specific environmental-dependent regulation. Here we revealed the distinct regulatory states formed in each pair of skeletal rods that apparently control rod-specific gene expression (Figure 9A). Interestingly, the cells at the tips of the postoral and anterolateral rods express the highest number of signaling molecules, FGF, FGFR2, and VEGFR2. Furthermore, the ligand VEGF is secreted from the ectodermal cells located next to the tips of these rods. Possibly the VEGF and FGF pathways drive and guide the cell migration required for the growth of postoral and anterolateral skeletal rods. Thus, the rod-specific GRNs are probably controlling the timing and growth rates of each pair of rods according to distinct developmental and environmental cues.

Our findings indicate that the role of VEGF signaling in sea urchin skeletogenesis has two distinct phases, in agreement with previous studies.[16,21-23] Early VEGF signaling is a key to the spatial organization of the skeletogenic cells, to the initial formation of the spicules, and to the expression of regulatory and differentiation genes at the ventrolateral cell clusters.[16,21,22] Yet, after the skeletogenic cells form the dorsal, ventral, and longitudinal chains and generate the tri-radiate spicules, the elongation of body, the mid-ventral, and the proximal part of the anterolateral rods, do not require VEGF signaling (Figures 2 and 3[16,21,23]). After spicule formation, VEGF signaling is required for the migration of the cells that form the postoral rods and the distal part of the anterolateral rods and for the expression of regulatory genes at the tips of the postoral rods, including the transcription factors, myoD1 and pitx1 (Figure 9B).

The sharp transition between the initiation and the elongation stage could suggest that early VEGF signaling controls cellular organizations essential for the formation of the spicule cavity. As mentioned above, the cells that build the body, proximal anterolateral and mid-ventral rods are positioned in their proper location and are connected through the pseudopodia cable at the time of the addition of VEGFR inhibitor in the late inhibition (25 hpf, Figure 1A,I[21]). The distal anterolateral rods and postoral rods are the only rods that grow without a pre-existing pseudopodia cable, which could suggest that VEGF activity is required to grow new spicule cavity. Thus, early VEGF signaling is required for the initiation of the spicule cavity in the lateral skeletogenic cell clusters, and late VEGF signaling is essential for the generation of the postoral and distal anterolateral rods, possibly due to VEGF unique role in cell migration and cavity formation (Figure 9B).

The expression of the genes encoding the transcription factors, MyoD1 and Pitx1 is dependent on VEGF signaling throughout skeletogenesis and they are a part of the postoral specific regulatory state (Figure 9A). The expression of myoD1 and pitx1 initiates at the skeletogenic cell clusters downstream of VEGF signaling at the time of spicule formation.[7] At late gastrulation, the expression of these genes is localized in the skeletogenic cell clusters and their vicinity, and later it is observed in the migrating cells that form the postoral rods (Figure 5). Late inhibition of VEGFR activity completely abolishes the expression of myoD1 and pitx1 at all tested time points (Figures 3-5). Thus, VEGF signaling is essential for the dynamic expression of myoD1 and pitx1 throughout skeletogenesis, first in the ventrolateral clusters and later at the tips of the growing postoral rods.

The knockdown of Pitx1 results in a significant delay in the growth of all skeletal rods (Figure 7), and downregulates the expression of some of VEGF targets (Figure 8 and 9B). The reduction of the expression level of Pitx1 targets in pitx1 morphants is more significant at 2 dpf than at 30 hpf (Figure 8C,L). At both time points the spatial expression of pitx1 is more localized than the broad expression of its target genes, SM30 and SM50, and the spatial expression of these genes is unchanged under Pitx1 knockdown (Figure 8D-I,M-R). As the skeletogenic cells are connected in a syncytium it is possible that Pitx1 protein migrates to neighboring cells and activates genes in the vicinity of pitx1 expressing cells. However, it is unlikely that at 2 dpf, when pitx1 is localized to the tips of the postoral rods, it regulates the broad expression of SM30 or the expression of SM50 at the tips of the anterolateral and body rods (Figure 9). Probably, the observed reduction of SM30 and SM50 levels and the size reduction in all skeletal rods are due to the role of Pitx1 in regulating gene expression at the ventrolateral cell clusters during the late gastrula stage, and not because of its late localized expression in the pluteus. To study the late role of Pitx1 in regulating gene expression at the tips of the postoral rods, a late perturbation technique is required, which is beyond the scope of this work.

The common participation of sea urchin Pl-Pitx1 and vertebrates' Pitx2 in biomineralization, makes it interesting to compare these two developmental programs. Pitx2 regulates vertebrate teeth development from bud

formation up until generation of enamel.[57,58] To the best of our knowledge, Pitx2 is not regulated by VEGF signaling during vertebrates' tooth development. Vertebrates' Pitx2 is one of the earliest genes specifically expressed in the oral ectoderm, where it is activated by FGF signaling and repressed by BMP signaling.[34] Sea urchin BMP signaling is important for skeletal patterning as it represses VEGF and VEGFR expression.[59] Other transcription factors that regulate tooth organogenesis such as, Dlx, Msx, Irx, and FoxJ1[35,57,58,60] are not involved in the regulation of skeletogenesis in the sea urchin embryo and are a part of the GRNs that control dorsal ectoderm specification.[61,62] Overall, there are more differences than similarities between the mesodermal GRN that regulates sea urchin skeletogenesis and the ectodermal GRN that drives vertebrate enamel formation, implying that these two GRNs do not have a common evolutionary origin.

Interestingly, the transcription factors, Pitx2 and MyoD, are a part of the GRN that controls skeletal muscle differentiation in vertebrates.[42] Specifically, Pitx2 activates the expression of *myoD* in limb muscle precursors through direct binding to MyoD core enhancer.[63] Moreover, Pitx2 and MyoD co-regulate the differentiation of all skeletal muscles, including limb, myotome, extraocular and pharyngeal arch muscles.[63] As discussed above, in the sea urchin embryo, *pitx1* and *myoD1* are co-expressed in the skeletogenic cells at the tips of the post-oral rod (Figure 4) and Pitx1 activates *myoD1* expression (Figure 9B). Other sea urchin orthologs of Pitx and MyoD, *pitx2* and *myoD2*, are expressed in the non-skeletogenic mesodermal cells, and MyoD2 is a part of the myogenesis GRN.[64] Within the intense rewiring of the mesodermal derived GRNs, the apparent conservation of the Pitx-MyoD connection is quite remarkable. This could be an example of the "plug-in" concept, where a successful regulatory sub-circuit is inserted into various positions in the GRN hierarchy to drive diverse outcomes.[65]

3.1 | Experimental procedures

3.1.1 | Animal and embryos

Adult *Paracentrotous lividus* were obtained from the Institute of Oceanographic and Limnological Research (IOLR) in Eilat, Israel. The animals were kept in aquaria in a dedicated room, in artificial seawater (ASW) with a salinity of 39 ppt. Eggs and sperm were obtained by injection of 0.5 M KCl solution into the adult sea urchin species. Embryos were cultured at 18°C in 0.2 μ filtered ASW.

3.2 | Imaging

All embryos presented in this work were imaged by Zeiss Axioimager 2 and aligned in Photoshop CS6. Figures were made in Adobe Illustrator CS6.

3.3 | Axitinib (AG013736) treatment

A 5-mM stock solution of Axitinib (AG013736, Selleckchem, Houston, TX), was prepared by reconstituting the chemical in dimethylsulfoxide (DMSO). The embryos were treated with Axitinib at a final concentration of 150 nM. Control embryos were cultured in 150 nM solution of DMSO at no more than 0.1% (v/v).

3.4 | Whole mount in situ hybridization probe preparation

Total RNA of 30 hpf *P. lividus* embryos was used to generate cDNA using the High capacity cDNA RT Superscript II Invitrogen 18 064-024. cDNAs of the target genes were PCR amplified, ligated, and inserted into pGemT (Promega A3600) or pJet plasmids (Thermofisher Scientific K1231). Primer list is provided in Table S1. RNA DIG probes were generated using Roche DIG labeling kit (Catalogue Number 1277073910) and SP6 polymerase 10810274001 or T7 polymerase 10881767001 (Sigma-Aldrich).

3.5 | WMISH procedure

WMISH was performed as described in Reference 7. Briefly, embryos were fixed by 1-hour incubation in 2% paraformaldehyde (PFA) in 4°C, followed by an overnight incubation at 4% PFA at 4°C. Fixed embryos were washed three times in TBST buffer, once with hybridization buffer at room temperature, followed by pre-hybridization at 65°C for 1 hour. Probes were added to the hybridization buffer (0.3-1 ng/mL) and incubated overnight at 65°C. Probe was washed by hybridization buffer at 65°C twice, followed by addition of a 1:1 mix of the hybridization buffer and 2XSSCT. Embryos were then washed with 2XSSCT and 0.2XSSCT. Antibody staining was done similarly to,[7] that is, washes with MABT, followed by first blocking solution with 10 mg/mL BSA and second blocking solution with 1 mg/mL BSA and 10% sheep serum. Then the embryos were incubated with anti-DIG antibody solution buffer at 4°C overnight. The embryos were washed with MABT, followed by two washes with alkaline phosphate buffer. The embryos

were stained with staining Solution (10% dimethylformamide, 0.1 M Tris pH 9.5, 50 mM MgCl2, 0.1 M NaCl, 1 mM levamisole, 337 mg/mL NBT, 175 mg/mL BCIP) in room temperature until the color was visible. Staining was stopped with 50 mM EDTA in MABT buffer. The probes were stored in 50% MABT and 50% glycerol at 4°C.

3.6 | cDNA preparation for QPCR experiments

For VEGFR inhibition experiments, total RNA was extracted from >1000 sea urchin embryos in each condition using RNeasy Mini Kit (50) from QIAGEN (#74104). For injected embryos, total RNA was extracted from 150 to 200 injected sea urchin embryos in each condition using RNeasy Micro Kit (50) from QIAGEN (#74004). Both kits were used according to the kits′ protocol. DNase treatment on the column was done using RNase-Free DNase Set-Qiagen (50) (#79254). RNA was reverse-transcribed using the High Capacity cDNA RT kit, AB-4368814 (Applied Biosystems) following the manufacturer's instructions.

3.7 | Quantitative polymerase chain reaction

Quantitative polymerase chain reaction (QPCR) was carried out in triplicates using a 384CFX-real-time thermal cycler and SYBR Green FastMix (Quantabio 95 072-012, Beverly, MA). Reaction conditions were as follows: 95°C for 3 min (one cycle), followed by 95°C for 10 s, 55°C for 30 s (40 cycles). Dissociation analysis was performed at the end of each reaction to confirm the amplification specificity. Primer set for all tested genes were designed using Primer3Plus (http://www.bioinformatics.nl/cgi-bin/primer3plus/primer3plus.cgi/). A complete list of primer sequences used for the experiments is provided in Table S1.

3.8 | QPCR expression levels quantification and differential expression analysis

Changes in gene expression were measured under different conditions and at the same developmental stage. Relative expression of genes was calculated by $1.9^{-\Delta\Delta CT}$ method using Ubiquitin as an internal reference gene for normalization.[7,53]

3.9 | Pitx1 MO microinjection

Egg jelly coat was removed by changing the pH of the ASW to 5.3 by gradual addition of 1 M HCl. The eggs were incubated at pH 5.3 for 1 min. The pH was then risen to 8.0 by the addition of 1 mL of 1 M Tris-HCl solution-pH 8. The eggs were rolled onto the injection plates treated with 0.25% protamine sulfate solution and injected with an injection solution containing 0.12 M KCl, 0.5 μg/μl Rhodamine Dextran, and 800 μM morpholino antisense oligonucleotide (MO). Down-regulation of *pitx1* was done by injecting two specific MOs targeting the splicing sites of the pre-mRNA. MOs were designed and synthesized by Gene Tools, Philomath, OR, according to *Pl-Pitx1* sequence. Splicing MO 1 (sMO1) was designed to remove the third exon, whereas sMO2 was designed to remove the second exon (Figure 6A). The sequences are as follows: sMO1: 5′-CACATAAATACTTACTCTAACTCGT-3′ and sMO2: 5′-GTACCTGAGATCGACAAGAAATTTA-3′.

Embryos injected with the same concentration of Random MO were used as control. Injected embryos were cultured at 18°C. At least three biological replicates, with different pairs of parents, were studied and imaged for each MO (see Table S2 for an exact number of embryos scored in each experiment).

3.10 | Quantification of skeletal length and statistical analysis

The lengths of skeletal rods were manually measured at 72 hpf using a built-in straight ruler tool in Zen software (Figure 7D). Embryos were flattened under the coverslip and the length of the rods was measured as shown in Figure 7D. The measurements were repeated for three biological repeats with a total of 109 embryos measured for sMO1, 99 embryos for sMO2, 115 embryos for Random MO in sMO1 experiment, and 99 embryos for Random MO in the sMO2 experiment. The data were analyzed in Excel and the statistical analysis was performed using Student's *t*-test in Excel and SPSS Statistics 21.

3.11 | Verification of the activity of pitx1 sMOs

The activity of the splicing MOs was checked by PCR reaction of cDNA prepared as described above from injected embryos collected at 44 hpf. All primers used for the splicing check can be found in Table S1. For sMO1,

the primer pair F1 + R1 was used (Figure 6A,B). The expected length of the PCR amplicon of the primers pair F1 + R1 in uninjected eggs (Un) and random MO (raMO) was approximately 480 bp, and the truncated amplicon in the *Pl-Pitx1* splicing sMO1 was 265 bp (excluding the third exon, Figure 6B). sMO2 was tested with a primer pair F2 + R2 (Figure 6A,C). The size of the expected amplicon for uninjected embryos and embryos injected with random MO was 819 bp, whereas the *Pl-Pitx1* sMO2 was expected to produce a truncated amplicon of 290 bp due to the deletion of the second exon (Figure 6C).

3.12 | Identification of putative Pitx1 bindings sites

We studied the promoter regions of SpSM30a and SpSM50 that were shown to drive expression in the skeletogenic cells[50,51,52] (Figure 8S,T). Putative binding sites were identified using the human and mouse Pitx1/2/3 position weight matrices (PWM) from Jasper, with a relative profile score of >80%. https://jaspar.genereg.net/analysis. Four putative Pitx binding sites are detected in the promoter region of SpSM30a and two putative Pitx binding sites are detected in the promoter region of SpSM50 (Figure 8S,T).

AUTHOR CONTRIBUTIONS
Kristina Tarsis: Conceptualization (equal); formal analysis (equal); investigation (lead); methodology (lead); validation (equal); visualization (equal); writing – original draft (equal); writing – review and editing (equal). **Tsvia Gildor:** Conceptualization (equal); formal analysis (equal); investigation (equal); methodology (equal); project administration (lead); supervision (equal); validation (lead); writing – review and editing (equal). **Miri Morgulis:** Formal analysis (supporting); investigation (supporting); methodology (supporting); visualization (supporting); writing – review and editing (equal). **Smadar Ben-Tabou de-Leon:** Conceptualization (equal); formal analysis (equal); funding acquisition (lead); investigation (equal); supervision (lead); visualization (equal); writing – original draft (equal); writing – review and editing (lead).

ORCID
Smadar Ben-Tabou de-Leon https://orcid.org/0000-0001-9497-4938

REFERENCES
1. Davidson EH. Emerging properties of animal gene regulatory networks. *Nature.* 2010;468(7326):911-920. doi:10.1038/nature09645
2. Olson EN. Gene regulatory networks in the evolution and development of the heart. *Science.* 2006;313(5795):1922-1927. doi:10.1126/science.1132292
3. O'Brien J, Hayder H, Zayed Y, Peng C. Overview of MicroRNA biogenesis, mechanisms of actions, and circulation. *Front Endocrinol (Lausanne).* 2018;9:402. doi:10.3389/fendo.2018.00402
4. De-Leon SBT, Davidson EH. Gene regulation: gene control network in development. *Annu Rev Biophys Biomol Struct.* 2007;36:191-212. doi:10.1146/annurev.biophys.35.040405.102002
5. Ettensohn CA. Encoding anatomy: developmental gene regulatory networks and morphogenesis. *Genesis.* 2013;51(6):383-409. doi:10.1002/dvg.22380
6. Oliveri P, Tu Q, Davidson EH. Global regulatory logic for specification of an embryonic cell lineage. *Proc Natl Acad Sci USA.* 2008;105(16):5955-5962. doi:10.1073/pnas.0711220105
7. Morgulis M, Gildor T, Roopin M, et al. Possible cooption of a VEGF-driven tubulogenesis program for biomineralization in echinoderms. *Proc Natl Acad Sci USA.* 2019;116(25):12353–12362. doi:10.1073/pnas.1902126116.
8. Rafiq K, Shashikant T, McManus CJ, Ettensohn CA. Genome-wide analysis of the skeletogenic gene regulatory network of sea urchins. *Development.* 2014;141(4):950-961. doi:10.1242/dev.105585
9. Piacentino ML, Zuch DT, Fishman J, et al. RNA-Seq identifies SPGs as a ventral skeletal patterning cue in sea urchins. *Development.* 2016;143(4):703-714. doi:10.1242/dev.129312
10. Yajima M, Umeda R, Fuchikami T, et al. Implication of HpEts in gene regulatory networks responsible for specification of sea urchin skeletogenic primary mesenchyme cells. *Zool Sci.* 2010;27(8):638-646. doi:10.2108/zsj.27.638
11. Sampilo NF, Stepicheva NA, Song JL. microRNA-31 regulates skeletogenesis by direct suppression of Eve and Wnt1. *Dev Biol.* 2021;472:98-114. doi:10.1016/j.ydbio.2021.01.008
12. Stepicheva NA, Song JL. microRNA-31 modulates skeletal patterning in the sea urchin embryo. *Development.* 2015;142(21):3769-3780. doi:10.1242/dev.127969
13. Gildor T, Winter MR, Layous M, Hijaze E, Ben-Tabou de Leon S. The biological regulation of sea urchin larval skeletogenesis: from genes to biomineralized tissue. *J Struct Biol.* 2021;213(4):107797 1-5. doi:10.1016/j.jsb.2021.107797.
14. Ettensohn CA, Kirrell DD. A member of the Ig-domain super-family of adhesion proteins, is essential for fusion of primary mesenchyme cells in the sea urchin embryo. *Dev Biol.* 2017;421(2):258-270. doi:10.1016/j.ydbio.2016.11.006
15. Duloquin L, Lhomond G, Gache C. Localized VEGF signaling from ectoderm to mesenchyme cells controls morphogenesis of

the sea urchin embryo skeleton. *Development*. 2007;134(12): 2293-2302. doi:10.1242/dev.005108

16. Adomako-Ankomah A, Ettensohn CA. Growth factor-mediated mesodermal cell guidance and skeletogenesis during sea urchin gastrulation. *Development*. 2013;140(20):4214-4225. doi:10.1242/dev.100479

17. Beniash E, Addadi L, Weiner S. Cellular control over spicule formation in sea urchin embryos: a structural approach. *J Struct Biol*. 1999;125(1):50-62. doi:10.1006/jsbi.1998.4081

18. Vidavsky N, Addadi S, Mahamid J, et al. Initial stages of calcium uptake and mineral deposition in sea urchin embryos. *Proc Natl Acad Sci USA*. 2014;111(1):39-44. doi:10.1073/pnas.1312833110

19. Vidavsky N, Addadi S, Schertel A, et al. Calcium transport into the cells of the sea urchin larva in relation to spicule formation. *Proc Natl Acad Sci USA*. 2016;113(45):12637-12642. doi:10.1073/pnas.1612017113.

20. Guss KA, Ettensohn CA. Skeletal morphogenesis in the sea urchin embryo: regulation of primary mesenchyme gene expression and skeletal rod growth by ectoderm-derived cues. *Development*. 1997;124(10):1899-1908.

21. Sun Z, Ettensohn CA. Signal-dependent regulation of the sea urchin skeletogenic gene regulatory network. *Gene Expr Patterns*. 2014;16(2):93-103. doi:10.1016/j.gep.2014.10.002

22. Morgulis M, Winter RM, Shternhell L, Gildor T, Ben-Tabou de Leon S. VEGF signaling activates the matrix metalloproteinases, MmpL7 and MmpL5 at the sites of active skeletal growth and MmpL7 regulates skeletal elongation. *Dev Biol*. 2021;473:80-89.

23. Chang WL, Su YH. Zygotic hypoxia-inducible factor alpha regulates spicule elongation in the sea urchin embryo. *Dev Biol*. 2022;484:63-74. doi:10.1016/j.ydbio.2022.02.004.

24. Ben-Tabou de Leon S. The evolution of biomineralization through the co-option of organic scaffold forming networks. *Cells*. 2022;11(3):1-23. doi:10.3390/cells11040595.

25. Morino Y, Koga H, Tachibana K, Shoguchi E, Kiyomoto M, Wada H. Heterochronic activation of VEGF signaling and the evolution of the skeleton in echinoderm pluteus larvae. *Evol Dev*. 2012;14(5):428-436. doi:10.1111/j.1525-142X.2012.00563.x

26. Gao F, Davidson EH. Transfer of a large gene regulatory apparatus to a new developmental address in echinoid evolution. *Proc Natl Acad Sci USA*. 2008;105(16):6091-6096. doi:10.1073/pnas.0801201105

27. Cary GA, Hinman VF. Echinoderm development and evolution in the post-genomic era. *Dev Biol*. 2017;427(2):203-211. doi:10.1016/j.ydbio.2017.02.003

28. Potente M, Gerhardt H, Carmeliet P. Basic and therapeutic aspects of angiogenesis. *Cell*. 2011;146(6):873-887. doi:10.1016/j.cell.2011.08.039

29. Tiozzo S, Voskoboynik A, Brown FD, De Tomaso AW. A conserved role of the VEGF pathway in angiogenesis of an ectodermally-derived vasculature. *Dev Biol*. 2008;315(1):243-255. doi:10.1016/j.ydbio.2007.12.035

30. Yoshida MA, Shigeno S, Tsuneki K, Furuya H. Squid vascular endothelial growth factor receptor: a shared molecular signature in the convergent evolution of closed circulatory systems. *Evol Dev*. 2010;12(1):25-33. doi:10.1111/j.1525-142X.2009.00388.x

31. Tettamanti G, Grimaldi A, Valvassori R, Rinaldi L, de Eguileor M. Vascular endothelial growth factor is involved in neoangiogenesis in *Hirudo medicinalis* (Annelida, Hirudinea). *Cytokine*. 2003;22(6):168-179.

32. Petit F, Sears KE, Ahituv N. Limb development: a paradigm of gene regulation. *Nat Rev Genet*. 2017;18(4):245-258. doi:10.1038/nrg.2016.167

33. Lin CR, Kioussi C, O'Connell S, et al. Pitx2 regulates lung asymmetry, cardiac positioning and pituitary and tooth morphogenesis. *Nature*. 1999;401(6750):279-282. doi:10.1038/45803

34. St Amand TR, Zhang Y, Semina EV, et al. Antagonistic signals between BMP4 and FGF8 define the expression of Pitx1 and Pitx2 in mouse tooth-forming anlage. *Dev Biol*. 2000;217(2):323-332. doi:10.1006/dbio.1999.9547

35. Green PD, Hjalt TA, Kirk DE, et al. Antagonistic regulation of Dlx2 expression by PITX2 and Msx2: implications for tooth development. *Gene Expr*. 2001;9(6):265-281. doi:10.3727/000000001783992515

36. Chan YF, Marks ME, Jones FC, et al. Adaptive evolution of pelvic reduction in sticklebacks by recurrent deletion of a Pitx1 enhancer. *Science*. 2010;327(5963):302-305. doi:10.1126/science.1182213

37. Duboc V, Logan MP. Pitx1 is necessary for normal initiation of hindlimb outgrowth through regulation of Tbx4 expression and shapes hindlimb morphologies via targeted growth control. *Development*. 2011;138(24):5301-5309. doi:10.1242/dev.074153

38. Gurnett CA, Alaee F, Kruse LM, et al. Asymmetric lower-limb malformations in individuals with homeobox PITX1 gene mutation. *Am J Hum Genet*. 2008;83(5):616-622. doi:10.1016/j.ajhg.2008.10.004

39. Logan M, Tabin CJ. Role of Pitx1 upstream of Tbx4 in specification of hindlimb identity. *Science*. 1999;283(5408):1736-1739.

40. Marcil A, Dumontier E, Chamberland M, Camper SA, Drouin J. Pitx1 and Pitx2 are required for development of hindlimb buds. *Development*. 2003;130(1):45-55.

41. Thompson AC, Capellini TD, Guenther CA, et al. A novel enhancer near the Pitx1 gene influences development and evolution of pelvic appendages in vertebrates. *eLife*. 2018;7:e38555. doi:10.7554/eLife.38555

42. Buckingham M, Rigby PW. Gene regulatory networks and transcriptional mechanisms that control myogenesis. *Dev Cell*. 2014;28(3):225-238. doi:10.1016/j.devcel.2013.12.020

43. Andrikou C, Iovene E, Rizzo F, Oliveri P, Arnone MI. Myogenesis in the sea urchin embryo: the molecular fingerprint of the myoblast precursors. *Evodevo*. 2013;4(1):33. doi:10.1186/2041-9139-4-33

44. Pieplow A, Dastaw M, Sakuma T, et al. CRISPR-Cas9 editing of non-coding genomic loci as a means of controlling gene expression in the sea urchin. *Dev Biol*. 2021;472:85-97. doi:10.1016/j.ydbio.2021.01.003

45. Ettensohn CA, Illies MR, Oliveri P, De Jong DL. Alx1, a member of the Cart1/Alx3/Alx4 subfamily of paired-class homeodomain proteins, is an essential component of the gene network controlling skeletogenic fate specification in the sea urchin embryo. *Development*. 2003;130(13):2917-2928.

46. Saunders LR, McClay DR. Sub-circuits of a gene regulatory network control a developmental epithelial-mesenchymal transition. *Development*. 2014;141(7):1503-1513. doi:10.1242/dev.101436

47. Röttinger E, Saudemont A, Duboc V, Besnardeau L, McClay D, Lepage T. FGF signals guide migration of mesenchymal cells,

control skeletal morphogenesis [corrected] and regulate gastrulation during sea urchin development. *Development*. 2008; 135(2):353-365. doi:10.1242/dev.014282

48. Killian CE, Croker L, Wilt FH. SpSM30 gene family expression patterns in embryonic and adult biomineralized tissues of the sea urchin, Strongylocentrotus purpuratus. *Gene Expr Patterns*. 2010;10(2–3):135-139. doi:10.1016/j.gep.2010.01.002

49. Mann K, Wilt FH, Poustka AJ. Proteomic analysis of sea urchin (Strongylocentrotus purpuratus) spicule matrix. *Proteome Sci*. 2010;8:33. doi:10.1186/1477-5956-8-33

50. Yamasu K, Wilt FH. Functional organization of DNA elements regulating SM30alpha, a spicule matrix gene of sea urchin embryos. *Dev Growth Differ*. 1999;41(1):81-91.

51. Makabe KW, Kirchhamer CV, Britten RJ, Davidson EH. Cis-regulatory control of the SM50 gene: an early marker of skeletogenic lineage specification in the sea urchin embryo. *Development*. 1995;121(7):1957-1970.

52. Arshinoff BI, Cary GA, Karimi K, et al. Echinobase: leveraging an extant model organism database to build a knowledgebase supporting research on the genomics and biology of echinoderms. *Nucleic Acids Research*. 2022;50(D1):D970-D979. doi:10.1093/nar/gkab1005

53. Gildor T, Ben-Tabou de-Leon S. Comparative study of regulatory circuits in two sea urchin species reveals tight control of timing and high conservation of expression dynamics. *PLoS Genet*. 2015;11(7):e1005435. doi:10.1371/journal.pgen.1005435

54. Malik A, Gildor T, Sher N, Layous M, Ben-Tabou de-Leon S. Parallel embryonic transcriptional programs evolve under distinct constraints and may enable morphological conservation amidst adaptation. *Dev Biol*. 2017;430(1):202-213. doi:10.1016/j.ydbio.2017.07.019

55. Erwin DH, Davidson EH. The evolution of hierarchical gene regulatory networks. *Nat Rev Genet*. 2009;10(2):141-148. doi:10.1038/nrg2499

56. Adams DK, Sewell MA, Angerer RC, Angerer LM. Rapid adaptation to food availability by a dopamine-mediated morphogenetic response. *Nat Commun*. 2011;2:592. doi:10.1038/ncomms1603

57. Venugopalan SR, Li X, Amen MA, et al. Hierarchical interactions of homeodomain and forkhead transcription factors in regulating odontogenic gene expression. *J Biol Chem*. 2011; 286(24):21372-21383. doi:10.1074/jbc.M111.252031

58. Bei M. Molecular genetics of tooth development. *Curr Opin Genet Dev*. 2009;19(5):504-510. doi:10.1016/j.gde.2009.09.002

59. Layous M, Khalaily L, Gildor T, Ben-Tabou de-Leon S. The tolerance to hypoxia is defined by a time-sensitive response of the gene regulatory network in sea urchin embryos. *bioRxiv*. 2021; 148(8):33795230. doi:10.1242/dev.195859

60. Yu W, Li X, Eliason S, et al. Irx1 regulates dental outer enamel epithelial and lung alveolar type II epithelial differentiation. *Dev Biol*. 2017;429(1):44-55. doi:10.1016/j.ydbio.2017.07.011

61. Ben-Tabou de-Leon S, Su YH, Lin KT, Li E, Davidson EH. Gene regulatory control in the sea urchin aboral ectoderm: spatial initiation, signaling inputs, and cell fate lockdown. *Dev Biol*. 2013;374(1):245-254. doi:10.1016/j.ydbio.2012.11.013

62. Saudemont A, Haillot E, Mekpoh F, et al. Ancestral regulatory circuits governing ectoderm patterning downstream of nodal and BMP2/4 revealed by gene regulatory network analysis in an echinoderm. *PLoS Genet*. 2010;6(12):e1001259. doi:10.1371/journal.pgen.1001259

63. L'Honore A, Ouimette JF, Lavertu-Jolin M, Drouin J. Pitx2 defines alternate pathways acting through MyoD during limb and somitic myogenesis. *Development*. 2010;137(22):3847-3856. doi:10.1242/dev.053421

64. Andrikou C, Pai CY, Su YH, Arnone MI. Logics and properties of a genetic regulatory program that drives embryonic muscle development in an echinoderm. *Elife*. 2015;4:e07343. doi:10.7554/eLife.07343

65. Peter IS, Davidson EH. Evolution of gene regulatory networks controlling body plan development. *Cell*. 2011;144(6):970-985. doi:10.1016/j.cell.2011.02.017

SUPPORTING INFORMATION

Additional supporting information may be found in the online version of the article at the publisher's website.